Reviews of Modern Plasma Physics (2022) 6:14
https://doi.org/10.1007/s41614-022-00074-4

SPECIAL TOPICS

Nonlinear evolution and control of neo-classical tearing mode in reversed magnetic shear tokamak plasmas

Wang Zheng-Xiong[1] · **Liu Tong**[1] · **Wei Lai**[1]

Received: 13 September 2021 / Accepted: 27 May 2022 / Published online: 3 July 2022

Abstract

The reversed magnetic shear (RMS) configuration is believed to be one of the most promising advanced scenarios to achieve steady-state operation in the future large-scale tokamak devices. Nevertheless, the neo-classical tearing mode (NTM) is a detrimental threat to the steady-state operation and should be appropriately controlled by various effective strategies. This paper reviews recent numerical results on the nonlinear evolution and control of NTMs in RMS tokamak plasmas. The numerical results are mainly obtained through running initial value code MHD@Dalian Code. First, the nonlinear features of TMs/NTMs with RMS are introduced in comparison with the tokamak experimental results. Then, several effective control strategies on NTMs and on NTMs triggering explosive bursts are reviewed, including differential plasma rotation, electron cyclotron current drive (ECCD) and resonant magnetic perturbation (RMP), as well as the synergistic effect of ECCD and RMP. The introduced strategies are all feasible and effective to prevent the explosive bursts under the proper operations of control techniques. Finally, a two-fluid model is adopted to investigate the effect of diamagnetic drift flow on the nonlinear properties of TMs/NTMs with RMS. The evolution features and their dependence on key plasma parameters, such as plasma resistivity, ion viscosity and parallel/perpendicular transport coefficients, are all investigated and analyzed in detail. Moreover, the prospects of potential future intense topics in this area are given in the last section.

Keywords Tokamak plasmas · Neo-classical tearing mode · Reversed magnetic shear

✉ Wang Zheng-Xiong
zxwang@dlut.edu.cn

[1] Key Laboratory of materials Modification by Beams of the Ministry of Education, School of Physics, Dalian University of Technology, Dalian 116024, China

1 Introduction

Steady-state operation is one of the key goals for operating large-scale advanced tokamak devices such as ITER and future fusion reactors (Gormezano et al. 2007). To achieve steady-state operation, the sustainability of high bootstrap current fraction is of great significance. The bootstrap current was theoretically predicted by Galeev et al. (Galeev 1968) and the possibility of steady-state operation in tokamaks with bootstrap current was first found by Bickerton et al. (Bickerton 1971). Kikuchi et al. have reviewed the experimental evidence for the bootstrap current in tokamaks (Kikuchi 1995). The bootstrap current, which is self-sustainable during the steady-state discharges, is an important part of the total plasma current. As a result of the toroidal geometry in tokamak magnetic configuration, the nonuniformity of the equilibrium magnetic field leads to a large amount of trapped particles moving in 'banana' orbit. The moving-forward particle lies in the inner side of the 'banana' orbit, while the moving-backward particle lies in the outer side. The existence of large radial pressure gradient ensures the net particle flux is in the direction of the total plasma current. Through diffusion in velocity space of the passing particles via collisions, the self-sustained bootstrap current can be generated. For the purpose of improving bootstrap current fraction, great efforts have been devoted into the relevant researches. Recent experiments in many different tokamaks have shown that during reversed magnetic shear (RMS) discharges, the formation of strong internal transport barriers (ITBs) can largely improve the confinement of plasma particle and energy (Ishida 1997; Fujita 2001; Crisanti 2002; Litaudon 2003; Greenfield 2004; Sakamoto 2005). In RMS configurations, ITBs are usually found to locate in the vicinity of the q_{min} position (Doyle et al. 2007). High bootstrap current could be driven in the vicinity of q_{min} position due to the formation of such strong ITBs, which in turn leads to larger shear reversal. Consequently, the loop results in a large fraction of bootstrap current, which makes RMS configuration one of the most promising advanced preforming scenarios to achieve steady-state operation. In the past decades, extensive efforts have been made to develop the fully noninductive operation, referring to the self-sustained bootstrap current effect. The pivotal feature is to optimize the current profile, on the purpose of enhancing core confinement and preventing instability of the plasma. Advanced scenarios with high performance obtained on different tokamaks could be categorized according to the adopted q-profile. There should exist a regime between the inductive and noninductive scenarios in which the current profile is externally modified but only partly driven by noninductive techniques. Generally, today's advanced experimental scenarios could be subdivided into three categories: zero or weakly RMS, moderately RMS and strongly RMS. Zero or weakly RMS, usually called a 'hybrid' scenario, is an intermediate step between monotonic and reversed shear operation (Kamada 1999; Sips 2002; Luce 2003). In this scenario, there are generally no ITBs in the core region of plasmas. Moderately RMS usually has a flat current profile and relatively low shear. In this scenario, ITBs in the core region usually exist. The discharges are often operated at reduced plasma current, maximizing the bootstrap current with

high performance (Ide 2000; Murakami 2003). This scenario is regarded as a good candidate for ITER steady-state operation. Strongly RMS deals with high bootstrap fraction plasmas. This scenario is of great importance for steady-state operation, especially for reactor-scale devices where the fraction of bootstrap current is required to be largely higher than 0.5. In this scenario, due to the strongly RMS, the current density near the magnetic axis can be very low and in certain cases even zero, often called 'current hole' (Fujita 2001; Sakamoto 2005; Shiraiwa 2004). In spite of these favorable features, there still exist severe issues required to be solved, such as magnetohydrodynamic (MHD) instability, fast particles confinement and higher current operation. In JT-60U experiments, RMS configuration discharges showed excellent confinement beyond breakeven point $Q_{DT}^{eq} = 1$ (Ishida 1997). Further experiments in JT-60U achieved bootstrap current fraction $f_b > 0.8$ under fully noninductive current drive (Fujita 2001) and also achieved longer duration of RMS steady-state discharges with high bootstrap current fraction $f_b \sim 0.75$ (Sakamoto 2005). Strongly RMS configurations are also extensively studied in view of ITER steady-state operation and the results show good prospects of RMS operations.

Due to the existence of ITBs in the RMS configuration, large pressure gradient often results in deleterious macroscopic MHD instabilities in a broad β_N region. MHD instabilities are big threats of destructing steady-state operation in advanced tokamak devices (Hender et al. 2007). It is found that the ITBs can cause ideal kink instabilities that would lead to disruptions in JT-60U (Takeji 2000), JET (Hender 2002), DIII-D (Turnbull 2002) and ASDEX Upgrade (Günter 2000). Unique to RMS configuration, there exits a $n = 1$ dominant mode with multiple harmonics, relating to a common limit to achieving the highest β. Through the analysis of ideal MHD stability, a $n = 1$ kink-ballooning mode is found to have a close β_N limit to the upper limit of the achievable β_N in experiments (Takeji 2000; Hender 2002; Turnbull 2002). The mode structure is covering a relatively wide region up to edge. In the advanced scenarios of present tokamaks, the resistive wall is usually applied to stabilize high β resulting in $n = 1$ kink mode. When there exists a resistive wall, an external kink, instead of being stabilized by a perfectly conducting wall, is reduced to a slow-growing resistive wall mode. Furthermore, under strong ITB condition, another ideal instability called the 'infernal' mode could be destabilized and coupled to ideal kink in the weak shear region, becoming the limit mechanism. Its mode structure have a maximum value in the vicinity of the q_{min}. It has been observed in some experiments that such instabilities led to disruptions. Both experiment and theory reveal that the β limit inversely changes with the peaking of the pressure profile. By means of pressure profile control, such disruptions could be prevented. Apart from these hard β-limiting ideal instabilities, the neo-classical tearing mode (NTM) was often found under a positive shear in certain cases, exerting a soft β limit. Thus, the resistive MHD instability, requiring the finite resistivity to be destabilized, is also very important. The tearing mode (TM), one of the most significant resistive MHD instabilities, is absorbing constant interest of intense researches in tokamak plasmas. The TM can break equilibrium magnetic topology due to the reconnection of magnetic field in the proximity of rational surface, during which the plasma resistivity plays an important role. The study on TM began in early 1960s. The scaling

law of the linear growth rate of TM on plasma resistivity η is first given by Furth et al. (Furth 1963) as $\gamma \propto \eta^{\frac{3}{5}}$. As the TM evolves with time, the mode soon enters into nonlinear phase called the Rutherford regime (Rutherford 1973). The temporal evolution of magnetic island width is determined according to the Rutherford equation by assuming constant ψ approximation. During the nonlinear phase of TM, the formation of macro-scale magnetic islands would badly degrade the effectiveness and efficiency of plasma confinement in core region and lead to the failure of discharges. In addition to the detrimentally dangerous classical TM, there exists another more deleterious MHD instability during high-β_N discharges, named NTM (Carrera 1986; Hegna 1992; Fitzpatrick 1995; Cai 2016). The excitation of NTMs is originated from the loss of equilibrium bootstrap current. Once there exists a 'seed' island, which could be provided by classical TM, the plasmas inside the magnetic islands are able to fast transport outwardly along the magnetic field lines, due to the fact that the transport coefficient in the direction along magnetic field lines is $8-10$ order larger than that in perpendicular direction. As a result, the pressure profile will be flattened inside the islands, which leads to the loss of bootstrap current and thus excites the NTM (Sauter 1997; Buttery 2001, 2003; Isayama 2001; La Haye 2000). Due to the usual large fraction of bootstrap current, the destruction of NTMs could be more detrimental during RMS discharges. Moreover, the nonmonotonic safety factor q-profile in RMS configurations leads to pairs of rational surfaces with same helicities. Such magnetic structure allows the perturbations on both rational surfaces to couple with each other and therefore reinforces the instability to form the double tearing mode (DTM) (Pritchett 1980; Wei 2011; Wang 2011; Wei 2011; Zhang 2019, 2020). As a consequence, the fast reconnection of magnetic field lines due to the existence of DTM might generate off-axis sawtooth phenomena and even lead to major disruptions (De Baar 1997; Günter 2000; Takeji 2002; Maget 2007; Zhang 2020), which could destroy reactor-scale tokamak devices like ITER. In consideration of the deleterious consequences that DTMs and NTMs may cause, it is imperatively necessary to investigate the evolution and control of DTMs and NTMs in RMS configurations.

Towards the aim of confinement improvement and disruption avoidance, plenty of useful techniques have been developed for the control of NTMs (La Haye 2006), such as differential plasma rotation (Liu 2021), externally applied resonant magnetic perturbation (RMP) (Yu 2000; Wang 2022), three-dimensional MHD spectroscopy (Wang 2019; Liu 2021) and electron cyclotron current drive (ECCD) (Maraschek 2007). In the early 1980s, theoretical studies had showed that it is possible to stabilize TM using radio frequency current drive and the feasibility of this method had also been predicted (Reiman 1983). In the late 1990s, the discovery of detrimental NTMs driven by bootstrap current led to a resurgence of relevant theoretical researches in the field of current drive (Hegna and Callen 1997; Zohm 1997). Due to its good property of localization, ECCD is suitable to be applied to control NTMs inducing magnetic islands without globally changing total plasma current profiles. In tokamak experiments, ECCD control experiments have been successfully implemented in ASDEX Upgrade (Gantenbein 2000), DIII-D (Prater 2003; Petty 2004) and JT-60U Isayama (2009). The experimental results demonstrate the feasibility and effectiveness of the stabilization on both $m/n = 2/1$ and $m/n = 3/2$ (with m

and n being poloidal and toroidal mode numbers, respectively) NTMs by ECCD, which are the most dangerous helicities. In ASDEX Upgrade RMS experiments, it has been shown for the first time in experiments that NTMs can be completely suppressed by applying co-ECCD (the EC driven current is parallel to the plasma current) (Gantenbein 2000). Generally, the required input power of EC wave for effectively suppressing NTM magnetic islands is of 10−20% as compared with the total heating power. After decades of numerical and experimental researches (Harvey 2001; Zohm 2001; Kamendje 2005; De Lazzari 2009; Bertelli 2011; Borgogno 2014; Fevrier 2016), ECCD is regarded as one of the most effective methods to stabilize the NTMs. For the control of NTMs by locally applied ECCD around resonant surfaces, there exist two main effects that matter. For one thing, the classical TM index Δ' could be modified by EC driven current $m/n = 0/0$ component. For another, the perturbed components of EC current directly counteract the perturbed bootstrap current near the vicinity of magnetic islands' O-points (Giruzzi 1999). In recent years, extensive numerical simulations and theoretical analyses have been carried out to investigate these effects of ECCD on NTM control (Yu 2004; Wang 2015; Liu 2020). Moreover, a number of reports have proposed that ECCD would play an integral part in the aspect of NTM control in the future ITER advanced scenario operations (Hayashi 2004; Zohm 2007; La Haye 2008).

Due to the excellent confinement properties of RMS configurations and the destructive effects of NTMs on RMS operations, it is essential to investigate relevant topics of NTMs' control with RMS in the cause of confinement improvement and disruption avoidance. The control of NTMs under RMS configurations has attracted constant interest of intense studies and would be a key issue of tokamak plasmas in a long run. This review paper will mainly present the recent numerical studies in RMS configurations on the evolution properties and control strategies of NTMs. The results are mainly obtained from simulation results of MHD@Dalian Code (MDC) (Wang 2015). The remainder of this paper is structured as follows. The modeling equations are introduced in Sect. 2. Section 3 presents the evolution behaviors of NTMs in RMS configurations. Several control strategies for stabilizing RMS NTMs and for preventing NTMs triggering explosive bursts to avoid major disruptions are reported in Sect. 4. Section 5 shows results of two-fluid effects on the evolution of RMS NTMs and the suppressive effect of diamagnetic drift flows on the explosive bursts. In the last section, the summary and discussion are given.

2 Modeling equations in MHD@Dalian

Considering the numerical results introduced in this review paper are mainly obtained via MDC, the modeling equations in MDC are described here. The MDC is an initial value code solving reduced MHD equations including bootstrap current effect, ECCD effect, RMP effect, shear flow effect and some double fluid effects. The finite difference method is applied in the radial direction. An ideally conducting wall is assumed as the boundary condition in the radial direction. The pseudo-spectral method and periodic boundary condition are applied in the poloidal and axial directions. The two-step

predictor–corrector method is applied in time advancement. Moreover, the MDC has been repeatedly benchmarked with the codes employed in (Yu 2000; Sato 2005).

2.1 Modeling for nonlinear evolution of neo-classical tearing mode

A set of reduced MHD equations in cylindrical geometry (r,θ,z) is employed to simulate the nonlinear evolution of NTMs. The normalized equations can be written as

$$\frac{\partial \psi}{\partial t} = [\psi, \phi] - \partial_z \phi - S_A^{-1}(j - j_b - j_d) + E_{z0}, \tag{1}$$

$$\frac{\partial u}{\partial t} = [u, \phi] + [j, \psi] + \partial_z j + R^{-1}\nabla_\perp^2 u, \tag{2}$$

$$\frac{\partial p}{\partial t} = [p, \phi] + \chi_\parallel \nabla_\parallel^2 p + \chi_\perp \nabla_\perp^2 p + S_0, \tag{3}$$

where ψ and ϕ represent magnetic flux and stream function, respectively. $j = -\nabla_\perp^2 \psi$ and $u = \nabla_\perp^2 \phi$ denote plasma current density and vorticity along the axial direction, respectively. p is plasma pressure. $j_b = -f\frac{\sqrt{\epsilon}}{B_\theta}\frac{\partial p}{\partial r}$ is bootstrap current density, where $f(r,\beta) = \int_0^a j_{b0} r dr / \int_0^a j_{z0} r dr$ is a function of radius r and plasma β measuring the strength of bootstrap current fraction, $\epsilon = a/R_0$ is the inverse aspect-ratio and B_θ is the poloidal magnetic field. The EC driven current density j_d nonlinearly evolves along the direction parallel to magnetic field lines. The behaviors of EC-driven current will be decided via another set of equations described in Sect. 2.3. The radial coordinate r is normalized by the plasma minor radius. Time t and velocity V are measured in units of Alfvén time $\tau_A = \sqrt{\mu_0 \rho} a / B_0$ and Alfvén velocity $V_A = B_0/\sqrt{\mu_0 \rho}$, respectively. $S_A = \tau_\eta / \tau_A$ and $R = \tau_\nu / \tau_A$ are the magnetic Reynolds number and Reynolds number, respectively, where $\tau_\eta = a^2 \mu_0 / \eta$ and $\tau_\nu = a^2/\nu$ are resistive diffusion time and viscosity diffusion time, respectively. $\chi_\parallel$ and $\chi_\perp$ denote the parallel and perpendicular transport coefficients, respectively, which are normalized by a^2/τ_A. The source terms $E_{z0} = S_A^{-1}(j_0 - j_{b0})$ and $S_0 = -\chi_\perp \nabla_\perp^2 p_0$ in Eqs. (1) and (3) are chosen to balance the diffusion of initial profile of ohmic current and pressure, respectively. The Poisson bracket is defined as $[f, g] = \hat{z} \cdot \nabla f \times \nabla g$. Each variable $f(r, \theta, z, t)$ in Eqs. (1)–(3) can be written in the form $f = f_0 + \tilde{f}(r, \theta, z, t)$ with f_0 and $\tilde{f}$ being the time-independent initial profile and the time-dependent perturbation, respectively. The perturbed fields can be Fourier-transformed as

$$\tilde{f}(r, \theta, z, t) = \frac{1}{2} \sum_{m,n} \tilde{f}_{m,n}(r, t) \exp(im\theta - inz/R_0) + c.c. \tag{4}$$

with R_0 being the major radius of the tokamak.

2.2 Modeling for double fluid effects

A reduced four-field equations is employed for modeling the nonlinear evolution of NTM including two-fluid effects under the assumption of constant electron temperature and cold ions (Ye 2019; Hu 2020). The normalized equations in cylindrical geometry (r,θ,z) can be written as

$$\frac{\partial u}{\partial t} = [u, \phi] + \frac{1}{n_{eq}}([j, \psi] + \partial_z j) + R^{-1}\nabla_\perp^2 u, \tag{5}$$

$$\frac{\partial \psi}{\partial t} = [\psi, \phi] - \partial_z \phi + V_{0*}\frac{1}{n_{eq}}\nabla_\parallel n - S_A^{-1}(j - j_b - j_d) + E_{z0}, \tag{6}$$

$$\frac{\partial n}{\partial t} = [n, \phi] - n_{eq}\nabla_\parallel v + 2\delta\nabla_\parallel j + D_\parallel \nabla_\parallel^2 n + D_\perp \nabla_\perp^2 n + S_0, \tag{7}$$

$$\frac{\partial v}{\partial t} = [v, \phi] + \frac{\beta_e}{2n_{eq}}\nabla_\parallel n + D_v \nabla_\perp^2 v, \tag{8}$$

Here, the same physics quantities as the last section will not be introduced again. In this model, the bootstrap current is calculated by electron density n expressed as $j_b = -f\frac{\sqrt{\epsilon}}{B_\theta}\frac{\partial n}{\partial r}$, where $f(r,\beta) = \int_0^a j_{b0} r dr / \int_0^a j_{z0} r dr$ is a function of radius r and plasma β measuring the strength of bootstrap current fraction, $\epsilon = a/R_0$ is the inverse aspect-ratio and B_θ is the poloidal magnetic field. v denotes parallel ion flow. n_{eq} is the equilibrium density profile normalized by the on-axis density n_0. $D_\parallel$ and $D_\perp$ denote the parallel and perpendicular transport coefficients, respectively, which are normalized by a^2/τ_A. The source term $S_0 = -D_\perp \nabla_\perp^2 n_0$ in Eq. (7) is chosen to balance the diffusion of initial electron density profiles. $\beta_e = 2\mu_0 n_0 T_e / B_0^2$ is the ratio of the kinetic pressure to magnetic pressure measured in the plasma center, where T_e is the constant electron temperature. $\delta = (2\omega_{ci}\tau_A)^{-1}$ is the ion skin depth, with $\omega_{ci} = eB_0/m_i$ being the ion cyclotron frequency. The ion Larmor radius is relevant to $(\rho_i/a)^2 = 2\beta_e\delta^2$. The diamagnetic drift velocity profile is $V_*(r) = V_{0*}/f_{dn}(r)$ with $V_{0*} = \delta\beta_e$ and $f_{dn}(r) = n_{eq}/(dn_{eq}/dr)$ being the profile of the normalized characteristic length of the plasma density.

2.3 Modeling for electron cyclotron current drive

In the MDC, a closure relation in (Westerhof 2014) is employed for the modeling of EC-driven current j_d, which is coupled into the reduced MHD model through the modified Ohm's law. The relation is mainly originated from the Fisch–Boozer effect and effectively represents the nonlocal character of the EC-driven current. The generation of this 'Fisch–Boozer' current can be briefly described as follows. The EC waves can cause a perturbation in velocity space localized at the resonant parallel

velocity. The perturbation is characterized by a bulge of electrons at supra-thermal perpendicular velocities and a hole at sub-thermal perpendicular velocities. Then, the perturbation will be convected along the magnetic field line out of the EC wave deposition region with the parallel velocity of the resonant electrons. Due to the existence of the collision, the hole and bulge in velocity space will gradually disappear with time. Since the collision frequency depends on the magnitude of velocity, the velocity space hole at low velocities is filled in more quickly than the bulge at high velocities' decays. As a result, a net current generates. The nonlinear evolution of the EC-driven current can be represented by the equations as

$$\frac{\partial j_{d1}}{\partial t} = - J_{d0} - \nu_1 j_{d1} + v_{pres} \nabla_{\parallel} j_{d1}, \tag{9}$$

$$\frac{\partial j_{d2}}{\partial t} = J_{d0} - \nu_2 j_{d2} + v_{pres} \nabla_{\parallel} j_{d2}, \tag{10}$$

$$j_d = j_{d1} + j_{d2}, \tag{11}$$

where j_{d1} and j_{d2} represent the perturbed current density driven by EC wave through the velocity space hole filling in and the bulge decaying, respectively. j_d is the net EC-driven current density. ν_1 and ν_2 denote the collision frequencies during the velocity space hole filling in and the bulge decaying, respectively. v_{pres} represents the velocity of parallel resonant electrons. Collision frequencies ν_1 (ν_2) and velocity v_{pres} are measured in units of Alfvén time $\tau_A = \sqrt{\mu_0 \rho} a / B_0$ and Alfvén velocity $V_A = B_0 / \sqrt{\mu_0 \rho}$, respectively. The source term J_{d0} in Eqs. (9) and (12) with opposite signs is the balance between two current density perturbations driven in opposite directions. And the form of J_{d0} is adopted with Gaussian distributions in both radial direction and helical angle direction as follows:

$$J_{d0} = j_{d0} exp \left\{ -4 \left[\left(\frac{r - r_0}{\Delta r_d} \right)^2 + \left(\frac{\xi - \xi_0}{\Delta \xi_d} \right)^2 \right] \right\}, \tag{12}$$

where j_{d0} is the magnitude of the source. r_0 and ξ_0 are the deposition region center of radial direction and helical angle direction, respectively. Δr_d and $\Delta \xi_d$ represent the deposition region width of radial direction and helical angle direction, respectively.

3 Nonlinear evolution of (neo-)classical tearing mode in reversed magnetic shear configurations

In the year of 1996, off-axis sawteeth had been observed in the Tokamak Fusion Test Reactor (TFTR) RMS experiments (Chang 1996). The off-axis sawteeth was considered as a result of the nonlinear evolution of the $m/n = 2/1$ DTM after compared with the numerical simulation results. The $m/n = 2/1$ mode is responsible for the off-axis sawtooth crashes and four distinguishable phases are found during the evolution of the mode, which is in agreement with the experimental results. In a

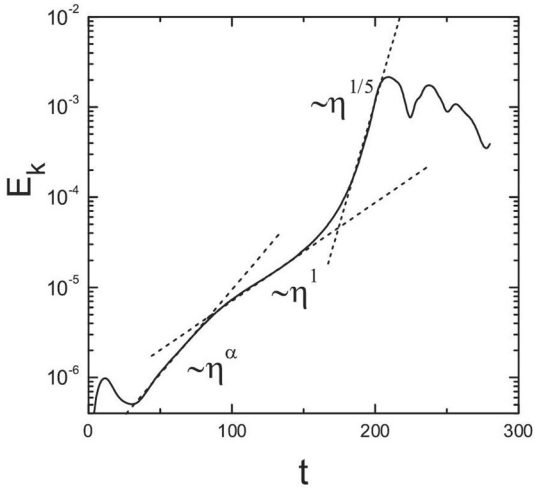

Fig. 1 Temporal evolution of the plasma kinetic energy. Reprinted from (Wang 2007)

2D geometry simulation, Wang et al. found similar results in a more general regime (Wang 2007). The phases include the linear growth phase, the slow nonlinear reconnection phase, the sawtooth crash phase, and the final decay phase. As shown in Fig. 1, the early growth phase belongs to linear phase. The second phase pertains to slow Rutherford transition phase with the $\gamma \propto \eta$ scale Waelbroeck (1993). After the separatrices of the magnetic islands merging together, the fast growth phase with the $\gamma \propto \eta^{\frac{1}{5}}$ scale occurs. The equivalent boundary inward flow drive could be used for understanding this fast growth (Wang 1996). Finally, at the end of the decay phase, all the field lines between the two resonant surfaces completely reconnected to finish the reconnection process, which can be seen in Fig. 2(d). Based on simulation results, a general criterion that predicts the final magnetic reconnection state for multiple resonant surfaces systems can be deduced. The final state of magnetic reconnection with even (or odd) numbers of the resonant surfaces is corresponding to nearly parallel field lines (or a single magnetic island).

As experimental discharges in early tokamak devices such as TFTR were limited to short-pulse type, the aforementioned experimental and numerical researches only focused on the early linear phase, the slow Rutherford phase, and the first burst-and-decay process (Chang 1996; Wang 2007). Nevertheless, after the decay triggered by the fast reconnection, the subsequent evolution behavior of plasmas yet remains to be further investigated. Considering that the steady-state operation is the ultimate objective for RMS scenarios in advanced reactor-scale tokamak devices such as ITER and future fusion reactors, the behaviors of plasmas for a very long duration of confinement are imperatively required to be obtained. By adopting nonlinear resistive MHD simulations (modeling in Sect. 2.1) during a very long evolution, Wei et al. discover a type of violent intermittent bursts induced by self-organized DTM reconnection in advanced RMS tokamak configurations (Wei and Wang 2014a). Figure 3 shows the temporal evolution of the perturbed energy. It could be observed that after the first explosive burst at $t = 5000\tau_A$ due to the drive of strong coupling between the islands, a series of periodic intermittent bursts onset at $t = 8000\tau_A$,

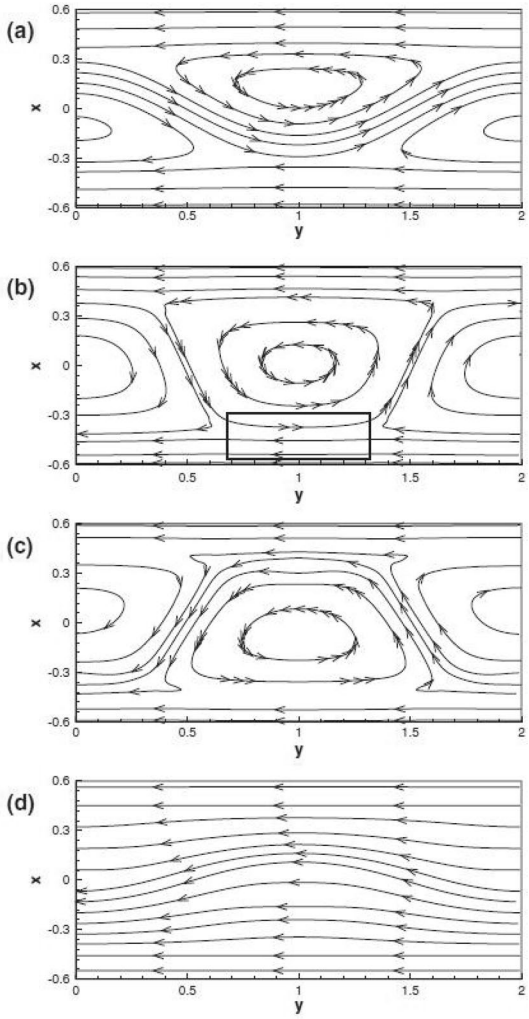

Fig. 2 The magnetic configurations at **a** $t = 184\tau_A$, **b** $t = 202\tau_A$, **c** $t = 210\tau_A$, and **d** $t = 280\tau_A$, respectively. Reprinted from (Wang 2007)

$t = 12000\tau_A$, $t = 17000\tau_A$, $t = 21000\tau_A$ and $t = 25000\tau_A$, which are novel properties compared to previous studies. Such intermittent violent rise of MHD activities due to the fast reconnection induced by self-organized DTM might continuously lead to annular sawtooth crashes, which can break the well-nested magnetic surfaces and thus badly influence the desired plasma confinement in steady-state RMS operations of future advanced tokamaks. The key process of such self-organized intermittent bursts localized at the off-axis region is similar to the situation of the typical on-axis sawtooth relaxation oscillation under positive magnetic shear. During the violent growth phase, the strong zonal field induced by nonlinear coupling of DTM quickly counteracts initial magnetic field, which makes the safety factor rise above 3 in the region between two resonant surfaces. As the resonant surfaces disappear, the mode

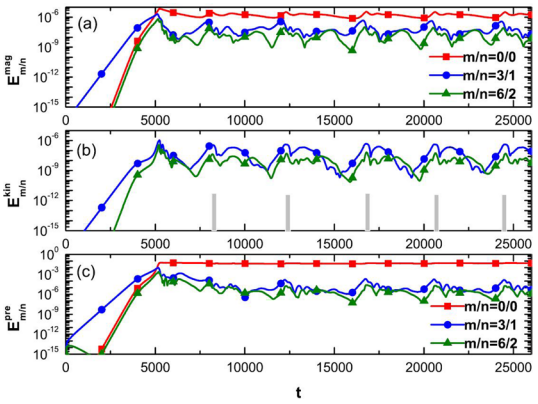

Fig. 3 Temporal evolution of the perturbed **a** magnetic energy, **b** kinetic energy, and **c** plasma pressure. The dark bars indicate the intermittent burst peaks. Reprinted from Wei and Wang (2014a)

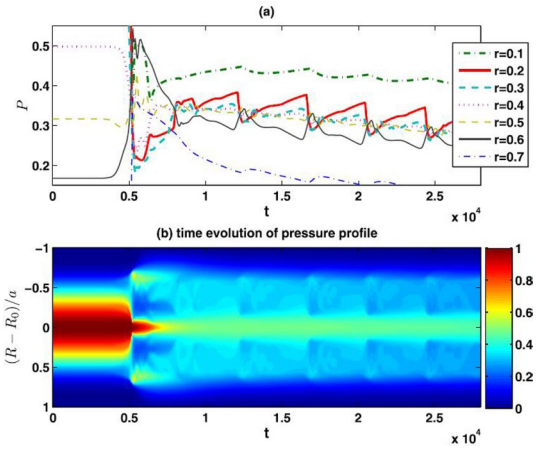

Fig. 4 **a** Temporal evolution of pressure values at different radial places. **b** Dynamic change of the pressure profile. Reprinted from (Wei and Wang 2014a)

consequently enters the decay phase under the influence of viscous damping effect. After the decay phase, the external energy source play an important part in the process of equilibrium reconstruction. Once the magnetic topology returns to the original RMS configuration, the system starts another round of the intermittent bursts and thus the loop continues. It is found in Fig. 4 that the pressure profile collapsed in the off-axis region after each round of the intermittent bursts, indicating the damage of confinement. Moreover, the period of these intermittent bursts increases with decreasing plasma resistivity found in Fig. 5.

Although single helicity simulations of DTM reconnection helps to understand the experimental phenomenon on some level, they did not include the coupling effect of perturbations on different rational surfaces with different helicities. Taking into account the coupling effect of multiple helicities, Wei et al. investigated the nonlinear evolution of multiple helicity DTMs in several RMS configurations (Wei and Wang 2014b). It is reported that the nonlinear evolution properties of multi-helicity DTMs directly depend on their linear unstable spectrum and the free energy

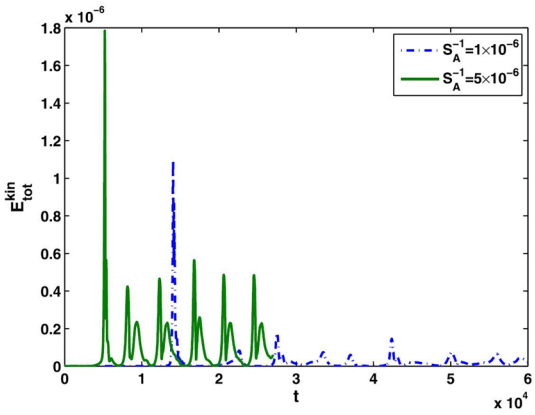

Fig. 5 Temporal evolution of the total kinetic energies with different plasma resistivity. Reprinted from Wei and Wang (2014a)

amount. Under the situation that linear growth rates of the dominant helicity DTMs are much larger than that of other helicities, single helicity simulation results could involve main nonlinear physics of the multiple helicity simulations. Nonetheless, when linear growth rates of multi-helicity DTMs are comparable to one another, the release of free energy in sequence due to the magnetic field reconnections of multi-helicity DTMs on different pairs of resonant surfaces will lead to consecutive explosive bursts. Usually, the most unstable helical mode would cause the first violent burst and lead to a temporary saturation of the system at a low level. After

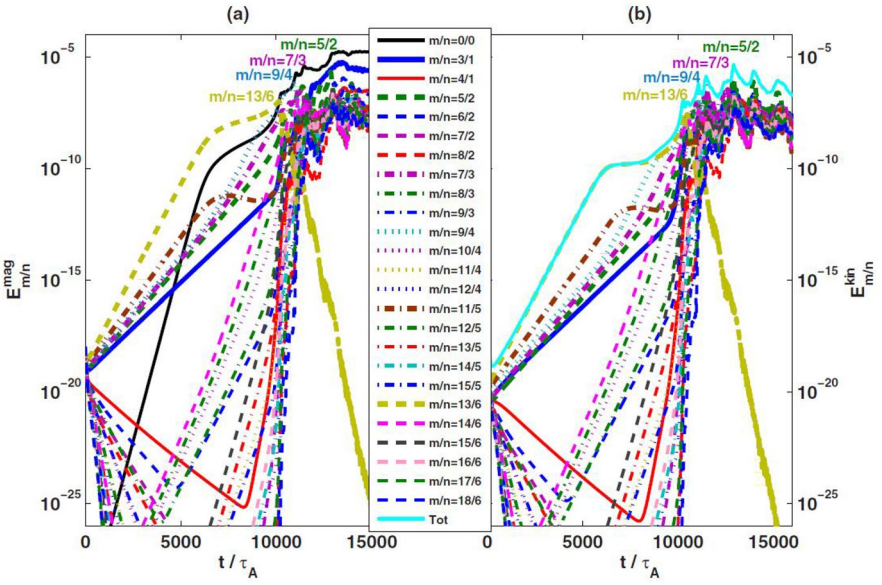

Fig. 6 Temporal evolution of **a** the magnetic energies and **b** kinetic energies for different harmonics in the very strongly RMS configuration. Reprinted from Wei and Wang (2014b)

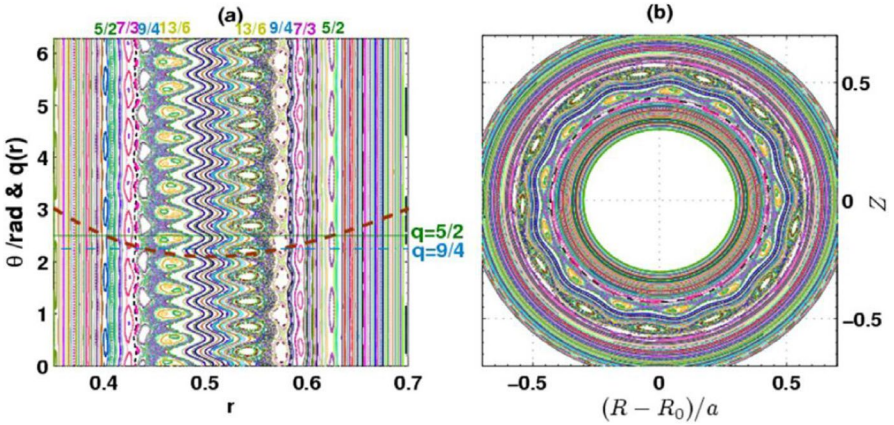

Fig. 7 Poincaré plot of magnetic field lines in a poloidal cross-section at $t = 8500\tau_A$ in the very strongly RMS configuration. Reprinted from (Wei and Wang 2014b)

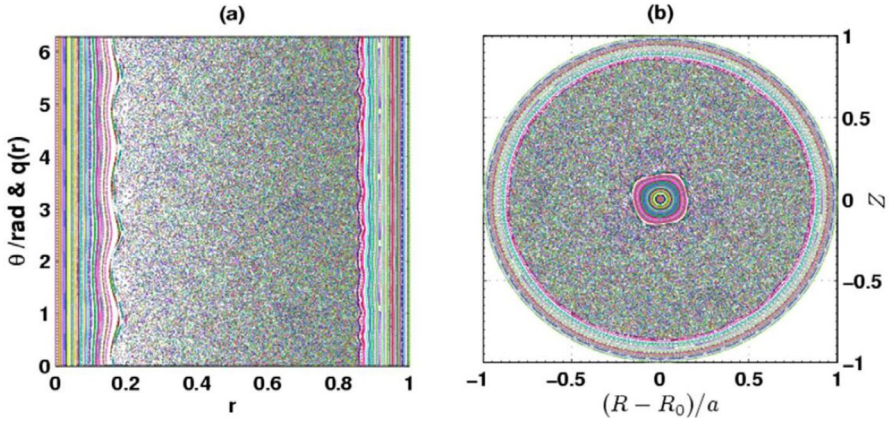

Fig. 8 Poincaré plot of magnetic field lines in a poloidal cross-section at $t = 13500\tau_A$ in the very strongly RMS configuration. Reprinted from (Wei and Wang 2014b)

a while, the second unstable helical mode could trigger the second burst due to the relatively smaller linear growth rate and relatively larger free energy that comes from equilibrium magnetic topology of that moment during the nonlinear evolution. Provided the linear growth rates of the rest helical modes are smaller and the free energy are larger than that of the helical modes of which the explosive bursts have already broken out, the consecutive bursts would continue. It is found in Fig. 6 that under a very strongly RMS configuration, the linear growth rates of several helicities of DTMs are comparable and thus a sequence of magnetic energy release lead to the successive bursts of the perturbed kinetic energy. It is clearly seen in Fig. 7 that at this moment the island chains with $m/n = 13/6$, 9/4, 7/3 and 5/2 can be found on the both sides, while the $m/n = 11/5$ island chains are not formed. And then

the continuous bursts happen one by one due to the strongly coupled $m/n = 9/4$, 7/3 and 5/2 DTM reconnections, respectively. At the final stage, the overlapping of the magnetic island chains ($m/n = 3/1$, 5/2, 7/3, 9/4, 13/6, etc.) during the evolution process of successive bursts induces the strong magnetic stochasticity at the off-axis region as displayed in Fig. 8. Such unique nonlinear behavior of multi-helicity DTMs cannot be observed by single helicity simulations.

Similar resistive MHD activities as in TFTR (Chang 1996) has also been observed during JT-60U RMS discharges with $m/n = 3/1$ mode being dominant. To make clear the physical characteristics of the MHD activities in JT-60U RMS experiments, Ishii et al. systematically investigated the DTMs' nonlinear evolution by adopting a group of initial q-profiles with different separations between the two rational surfaces. It is found that only in the intermediate separation cases, explosive bursts of the DTMs can happen after the Rutherford phase (Ishii 2000, 2002) displayed in Fig. 9. Janvier et al. further investigated the physical mechanism behind the triggering of the explosive burst (Janvier 2011). The asymmetrical flux-driven reconnection, due to the coupling of the DTM perturbations on both rational

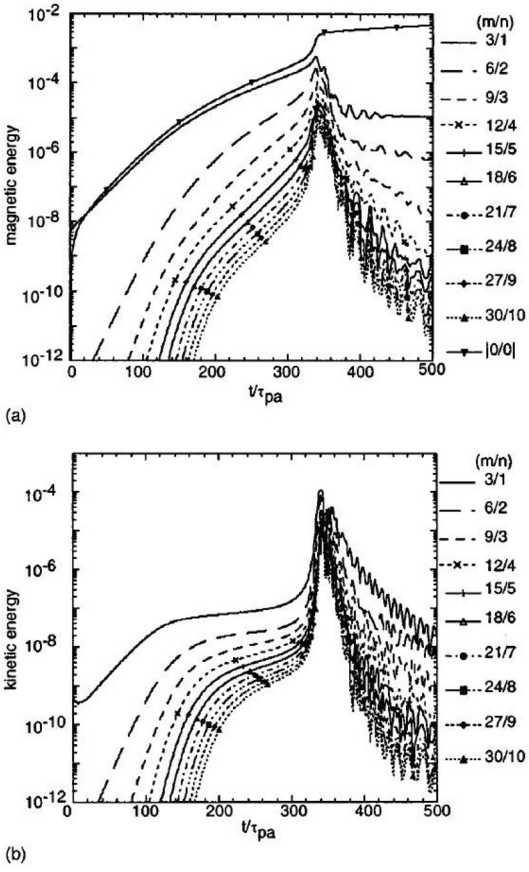

Fig. 9 Temporal evolution of the plasma perturbed **a** magnetic energy and **b** kinetic energy of DTM for different harmonics. Reprinted from Ishii (2000)

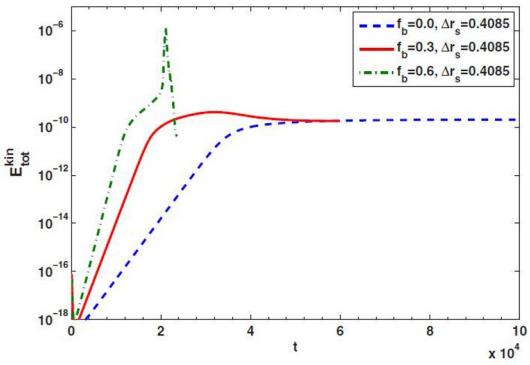

Fig. 10 Temporal evolution of the kinetic energy of DTMs for various bootstrap current fraction. Reprinted from Wang (2015)

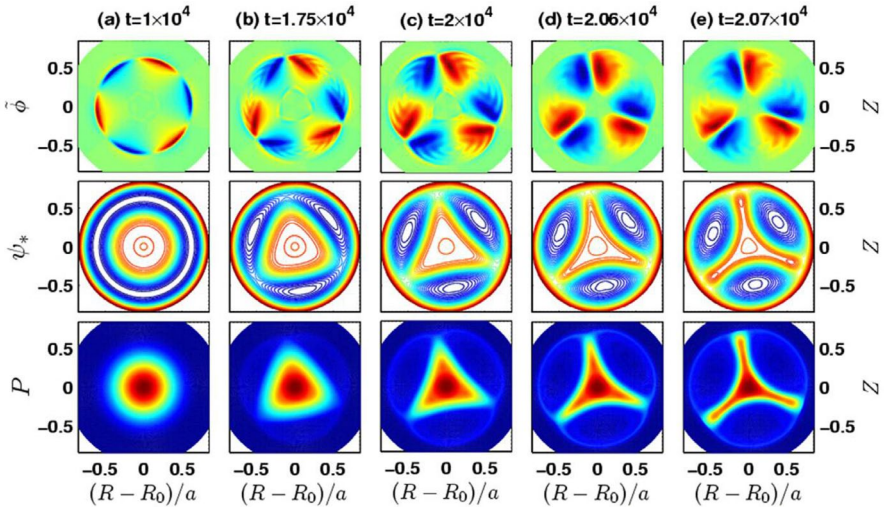

Fig. 11 Typical contours of potential (top row), helical magnetic flux (middle row) and pressure (bottom row) of the DTMs with $f_b = 0.6$. Reprinted from Wang (2015)

surfaces, deforms the structure of magnetic islands into a triangular shape. This type of explosive event of reconnection would happen as the level of the island triangular deformation is beyond a certain degree. Taking into account the effect of bootstrap current, Wang et al. found that explosive bursts could be induced even under the situation with an extremely large separation as long as the fraction of the bootstrap current is sufficiently high (Wang 2015). It is noted that the perturbed bootstrap current has a stabilizing effect on the inner islands and a destabilizing effect on the outer islands (Yu 1997; Yu and Günter 1999). The perturbed bootstrap current can be evaluated via the formula $j_b = -f\frac{\sqrt{\epsilon}}{B_\theta}\frac{\partial p}{\partial r}$ introduced in Sect. 2.1. Although the inner side is stabilized while considering bootstrap current effect, the explosive burst is still able to happen in large separation conditions with very high bootstrap current fraction, provided the destabilizing drive on outer side is overwhelming. Figure 10

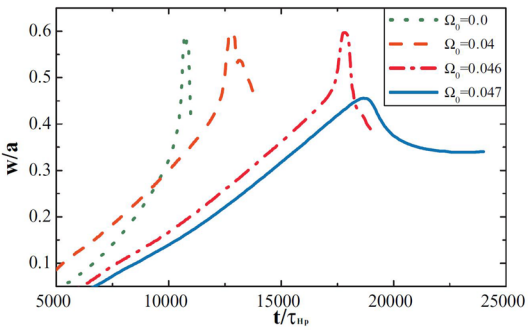

Fig. 12 Temporal evolution of the outer magnetic island width of the NTMs in the presence of differential rotations for $f_b = 0.3$. Reprinted from Wang (2017)

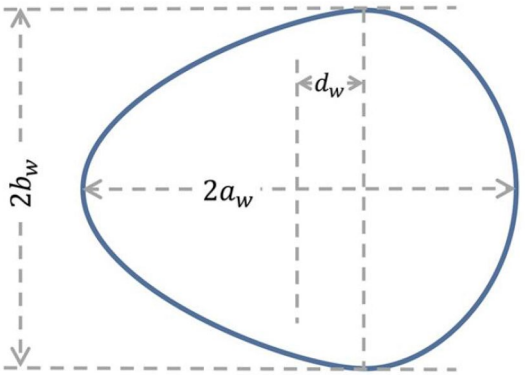

Fig. 13 Deformation of a magnetic island at outer rational surface. The definition of island elongation δ and triangularity κ is $\delta = |d_w/a_w|$ and $\kappa = |b_w/a_w|$, respectively. Reprinted from Wang (2017)

shows the temporal evolution of the kinetic energy of NTMs with various bootstrap current fractions. It is found that while the fraction is as large as $f_b = 0.6$, an explosive burst occurs, where other low fraction situations do not. The typical contours of key physical quantities are plotted in Fig. 11. Moreover, for small and intermediate separation conditions, the bootstrap current effect could also modify the nonlinear behaviors of DTM evolution to some extent.

4 Control of (neo-)classical tearing mode in reversed magnetic shear configurations

For the purpose of controlling NTMs in various RMS configurations, Wang et al. systematically investigated the effects of differential rotation on the nonlinear evolution of NTMs. In the simulation, the initial current profile is based on the equilibrium of JT-60U tokamak RMS experimental discharges (Wang 2017). It is found that the explosive burst can be effectively avoided by involving the differential rotation into nonlinear simulations even if the loss of equilibrium bootstrap current greatly strengthens the explosive bursts, which can be seen in Fig. 12. To effectively control NTMs, the shear location of the differential rotation is the pivotal factor. The differential rotation that has a strong shear located at the vicinity of outer resonant

surface can completely suppress the explosive burst in various RMS configurations, while located at other locations can not. To predict the onset of explosive burst in the conditions of high bootstrap current fraction and relatively small separations, a couple of measurable parameters are introduced to characterize the structure deformation of the magnetic islands right before the explosive bursts beak out, which denote the triangularity κ and elongation δ of the outer magnetic island. Figure 13 is a schematic diagram showing the definition of the measurable parameters. In experiments, the structure of islands can be obtained via electron cyclotron emission imaging (ECEI) diagnostic. The predicting effectiveness are displayed in Fig. 14. It is noted that, to investigate the effect of different fractions of bootstrap current, the initial bootstrap current is set to zero in the baseline simulation case. It is found that, before the explosive burst, there exist a clear inflection point in each parameter. However, with increasing bootstrap current fraction, the inflection point is gradually becoming ambiguous for the elongation and the magnetic island width. Among the three parameters, the triangularity is the most feasible and the most effective parameter in predicting the onset moment of the explosive burst. Moreover, the dependence of the critical triangularity on various plasma parameters is investigated and a database including threshold of triangularity in different plasma parameters is established based on numerical results, which should be further verified by experimental data in the future. On the basis of this database, a feasible way to avoid the occurrence of the explosive burst during RMS discharges could be brought forward. As the resolution of the ECEI diagnostic improves, the structure of the magnetic islands could be real time obtained with high precision. Thus, the instantaneous triangularity of the outer islands could be monitored in real time. After comparing the instantaneous

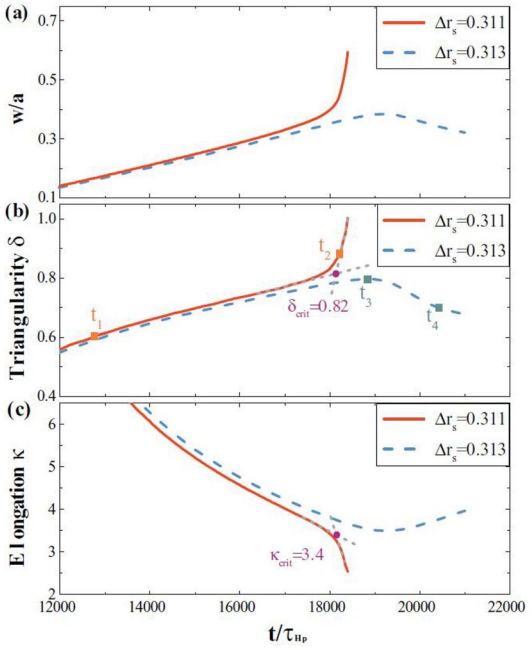

Fig. 14 Temporal evolution of **a** magnetic islands width and **b** triangularity δ and elongation κ of the DTM for $f_b = 0$ in the absence of rotation. The onset of explosive burst is estimated by the crossing point of two dashed lines. Reprinted from Wang (2017)

triangularity with the ones in pre-established database, the ECCD would be immediately switched on once the triangularity value approaches the warning line.

Among numbers of control techniques, the ECCD is generally considered as one of the most effective methods to suppress NTMs. By injecting EC wave, noninductive current can be driven around the vicinity of the magnetic islands' O-points along the plasma current direction, which can compensate the loss of equilibrium bootstrap current. Large amounts of studies are focusing on normal magnetic shear situations. As a promising candidate scenario for future advanced large-scale tokamaks, however, the control effectiveness under RMS configurations has not been systematically investigated yet. Motivated by these reasons, Liu et al. investigated the stabilization of NTMs and the NTMs triggering explosive bursts by ECCD (Liu 2018). It is found that the NTMs can be effectively stabilized by ECCD with sufficiently strong driven current and timely switch-on of ECCD. For classical situation, DTM could be easily stabilized with sufficient input power of ECCD. After considering the neo-classical current (i.e., bootstrap current) effect, the evolution of control process becomes complicated. The control of the NTMs is far more difficult than the classical situations. Figure 15 exhibits the temporal evolution of the outer magnetic island width under the application of ECCD aiming at the outer islands' O-points. The ECCD is turned on during the saturation phase of the neo-classical islands (i.e., magnetic islands destabilized by the loss of equilibrium bootstrap current). At the beginning of turning on ECCD, the width of the outer islands are effectively reduced. Nonetheless, instead of being completely suppressed, the outer islands precipitously grow after the occurrence of so called 'phase flip'. During the 'phase flip', the O-point and the X-point of the islands interchange with each other, and the island width is bouncing back from the bottom point. Soon after that, the explosive burst is triggered by the dramatically growth of NTMs. The key factor is the strong zonal magnetic field (i.e., perturbed $m/n = 0/0$ magnetic field) induced during the nonlinear evolution of NTMs. Since the strong zonal field can modify the magnetic topology, the deposition of EC-driven current is influenced after the ECCD is switched on. While the driven current inside the magnetic islands can modify the island structure and further influence the zonal field via nonlinear coupling. The

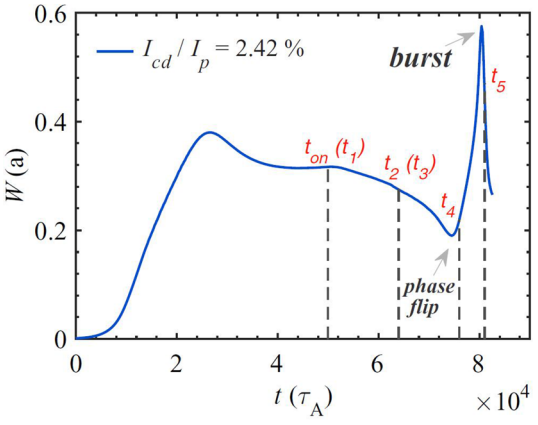

Fig. 15 Temporal evolution of the magnetic island width in the outer rational surface for bootstrap current fraction $f_b = 0.3$. Reprinted from Liu (2018)

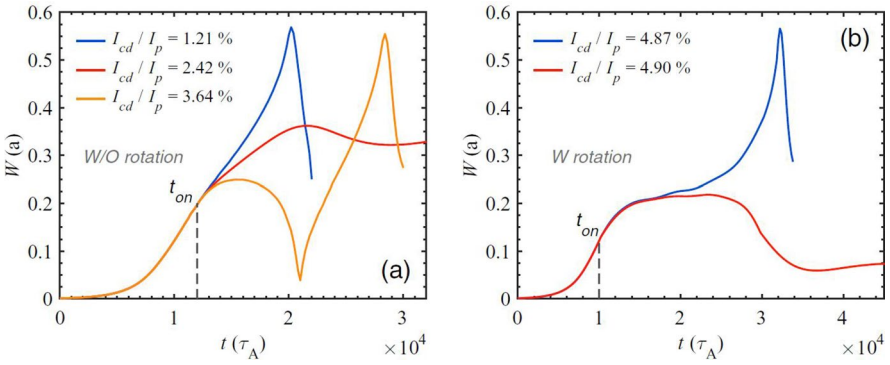

Fig. 16 Temporal evolution of the magnetic island width on the outer rational surface for different magnitudes of EC-driven current in the cases (**a**) without and **b** with plasma rotation. The bootstrap current fraction is $f_b = 0.6$. Reprinted from Liu (2018)

zonal field, driven current and magnetic islands make up a loop to interact with one another, resulting in the intense fluctuation of magnetic surfaces. As a consequence, the driven current cannot steady deposit. To avoid the strong zonal magnetic field, the ECCD is turned on as early as possible, which turns out to be feasible and effective to lower the influence of this intense fluctuation. Based on this idea, the explosive burst can also be effectively suppressed whether including plasma rotation or not, as shown in Fig. 16.

With the goal of further improving the stabilizing effectiveness and efficiency of ECCD, Tang et al. investigated the synergistic effects of RMP and ECCD on the NTMs' control under RMS configurations Tang (2020). To test the effect of RMP on NTMs' control without ECCD, the investigation is implemented under the condition of moderate separations. It is found in Fig. 17 that a sufficiently large rotating RMP is able to completely prevent the occurrence of the explosive bursts. Moreover, the rotating RMP would generate zonal flows with strong shear. Thus, a larger RMP is required to strengthen the penetration of the generated zonal flows. Otherwise, the applied RMP is not able to reach the resonant surface. To achieve this goal, the applied RMP is required to have an extremely large frequency. There exist two main reasons. One is that the velocity of RMP generating zonal flows is in positive proportion to the frequency of applied RMP. The other is that the NTMs are not prone to being locked under large frequency situations. Based on the properties of RMP control, the synergistic effects of RMP and ECCD are investigated. In the regime of large separations, the investigations are first focusing on the control of locked magnetic islands by static RMP and continuous ECCD displayed in Fig. 18. By applying different input power of ECCD, the NTMs can be suppressed to varying degrees including complete stabilization. The optimal radial aiming location of ECCD is a slightly inward deviation with respect to the initial outer resonant surface due to the deformation of the island structure during the interaction between the islands on both sides. Finally, synergistic effects of rotating RMP and modulated ECCD on the control of NTMs are investigated in the large separation. In present tokamaks, the typical thermal collision frequency is in an order of $10^{-3}\tau_A^{-1}$. Here, the collision frequency at low velocity and at high velocity are chosen

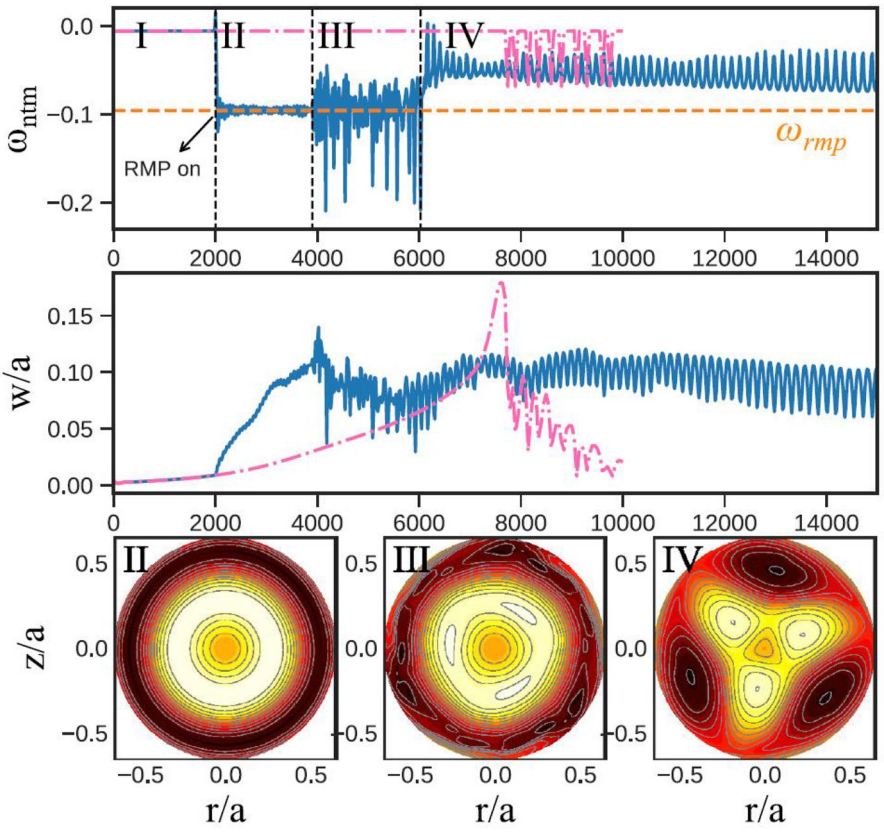

Fig. 17 Mode frequency and island width in a burst avoidance case (blue lines) compared with the case without RMP (pink lines). The input parameters are set as RMP frequency $\omega_{rmp} = -9.6 \times 10^{-2}$, RMP amplitude $\psi_{rmp} = 5 \times 10^{-4}$ and NTM frequency $\omega_{ntm} = -6 \times 10^{-3}$. The process can be divided into four phases. (I) Without RMP, the mode rotates at its natural frequency. (II) After RMP turning on, mode frequency locks to RMP soon. (III) Mode frequency starts to oscillate and the structure of magnetic islands are broken. (IV) Mode frequency maintains at lower level than RMP with little oscillation. Typical contour plots of helical magnetic flux with RMP in different regimes (II) $t = 2200\tau_A$, (III) $t = 4500\tau_A$ and (IV) $t = 12000\tau_A$ are given in the lower pictures. Reprinted from Tang (2020)

as $\nu_1 = 2.5 \times 10^{-3}\tau_A^{-1}$ and $\nu_2 = 5 \times 10^{-4}\tau_A^{-1}$, respectively. In the following simulations, the collision frequencies are fixed, and the rotation frequency of RMP will accordingly vary to adjust the ratio of rotation frequency and collision frequency. It is noted in Fig. 19 that decrease the ratio of rotation frequency and collision frequency of fast electrons could improve the ECCD effectiveness. For a lower RMP frequency, corresponding to approaching or moving away from the O-point of island, the deposited intensity of driven current can rise and fall rapidly in a modulation period. However, with large frequency, the driven current keeps almost constant with little oscillation due to the frequently turn-on and turn-off of the ECCD. Therefore, to obtain a better stabilizing effect for modulated ECCD in present tokamaks, a relatively slow rotating RMP should be applied to slow down the NTMs' rotation. Figure 20 shows the favorable effect of

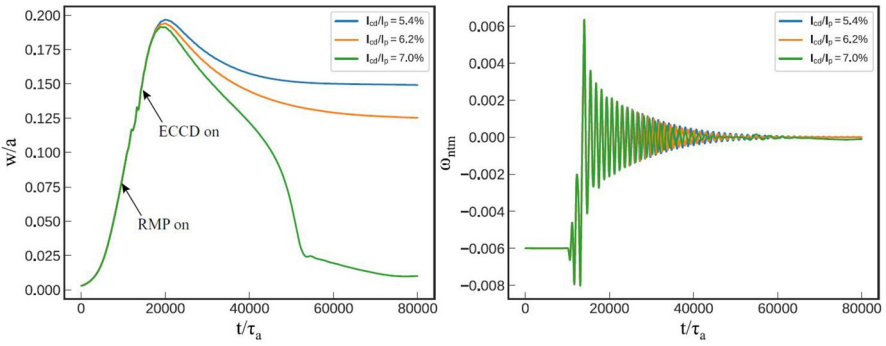

Fig. 18 Temporal evolution of island widths (left) and mode frequency (right) for different input power of ECCD. The ECCD is turned on after the islands are totally locked by a static RMP. Reprinted from Tang (2020)

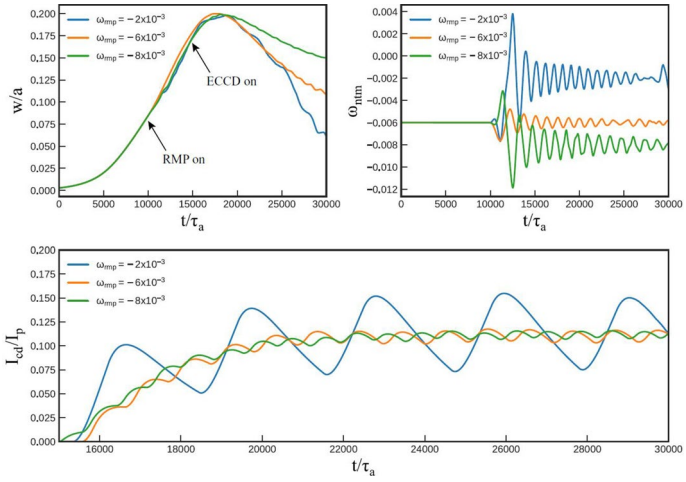

Fig. 19 Evolution of island width (upper left) and mode frequency (upper right) versus time for different RMP frequencies and the corresponding driven current fraction I_{cd}/I_p versus time (lower). The RMP is turned on at $t = 10000\tau_A$ and ECCD is switched on at $t = 15000\tau_A$ after the islands are totally locked by rotating RMP. Reprinted from Tang (2020)

the modulated ECCD. And the optimal on-duty ratio for modulated ECCD is in an order of $60 - 70\%$.

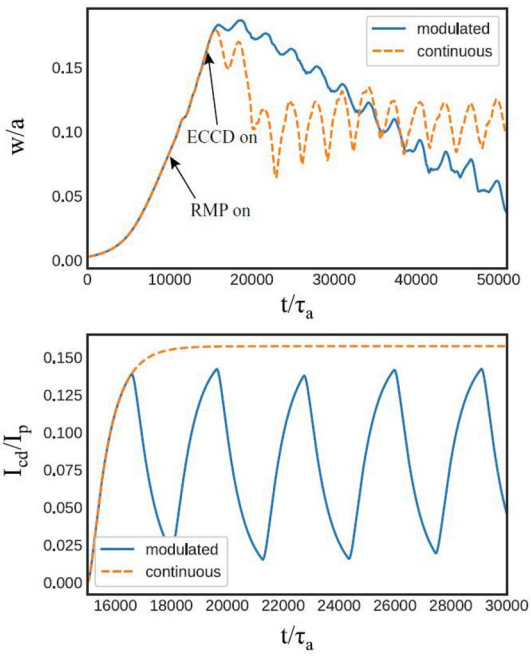

Fig. 20 Comparison of the temporal evolution of island width (upper) and driven current (lower) for modulated and continuous ECCD. Reprinted from Tang (2020)

5 Two-fluid effect on the nonlinear evolution of (neo-)classical tearing mode in reversed magnetic shear configurations

Although the single-fluid MHD model has made a considerable success for understanding the physical mechanism behind the MHD events in the area of fusion plasmas, there exist some extra physical effects that are not included but play important roles within certain range of plasma parameters. For instance, the effects of finite ion Larmor gyroradius and the parallel gradient of the electron pressure could not be simply neglected within the high temperature regime. In light of the aforementioned elucidation, Ye et al. investigated the diamagnetic drift effect on the nonlinear evolution of DTMs (Ye 2019) using a two-fluid drift-MHD model (Hazeltine 1985; Nishimura 2008; Li 2009; Uzawa 2010; Yu 2010; Hu 2014, 2016; Liu 2016) introduced in Sect. 2.2. In addition to the $E \times B$ velocity, the drift-MHD model reserves the drift velocity of the charged particles. It is found that the diamagnetic drift effect has a destabilizing effect on the Rutherford phase of DTMs' evolution. Nevertheless, the occurrence of the DTM explosive bursts can be effectively suppressed by the diamagnetic drift flow as displayed in Fig. 21. The δ is ion skin depth as introduced in Sect. 2.2, directly related to the strength of the diamagnetic drift flow. The δ needed to effectively avoid the explosive burst is defined as δ_c. The reason of the suppressing effect is that the difference of rotation frequency between the two rational surfaces can be enhanced while increasing the diamagnetic flow, which weakens the coupling effect between the DTMs' islands on both sides and thus suppress the explosive bursts. Figure 22 shows the radial profile of the total flow, zonal flow and electron diamagnetic flow during the Rutherford phase with

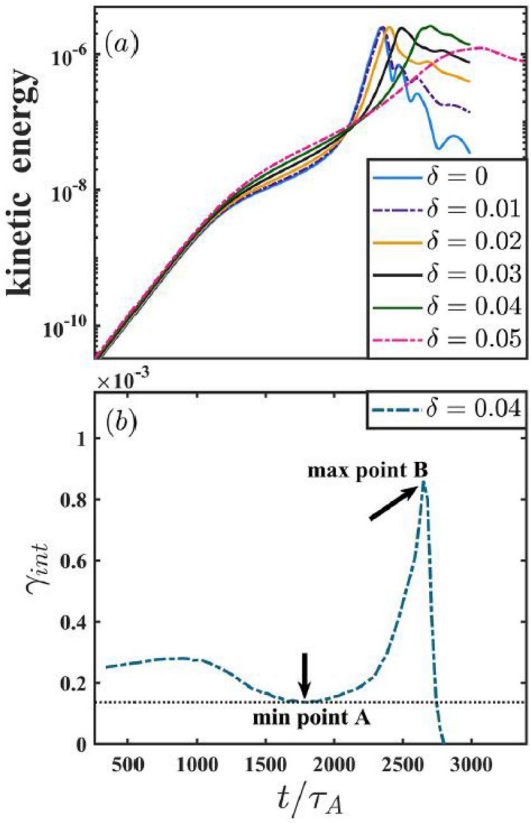

Fig. 21 **a** The evolutions of perturbed plasma kinetic energy for different δ. **b** The instantaneous growth rate of kinetic energy for $\delta = 0.04$ shown in the figure (a). Reprinted from Ye (2019)

different plasma resistivity. The red solid curves and the blue dotted curves represent the case with plasma resistivity $\eta = 5 \times 10^{-6}$ and $\eta = 1 \times 10^{-5}$, respectively. In the regime of low ion viscosity, increasing viscosity can increase the critical value δ_c, which means the stronger drift flow is required to avoid the explosive burst. The total difference of rotation frequency between the two rational surfaces, including both the $E \times B$ flow and the drift flow, determines the critical value. As viscosity increases, the total difference of rotation frequency is weakened during the Rutherford phase. Therefore, with no change of $E \times B$ flow, a stronger diamagnetic flow is favorable to maintain the relative rotation of islands on both sides. In the regime of large viscosity, the critical drift flow δ_c decreases as viscosity increases. The rotation frequencies on both sides are close to each other so that the total difference of rotation becomes negligible. Under this circumstance, the large viscosity itself would exert a extremely strong stabilizing effect on DTMs, which largely weakens the coupling effect between the islands on both sides. Thus, only a weak diamagnetic flow is required to suppress this kind of explosive bursts.

Focusing on the effect of two-fluid on NTMs under RMS configurations, Hu et al. extended the numerical model to include the bootstrap current terms and

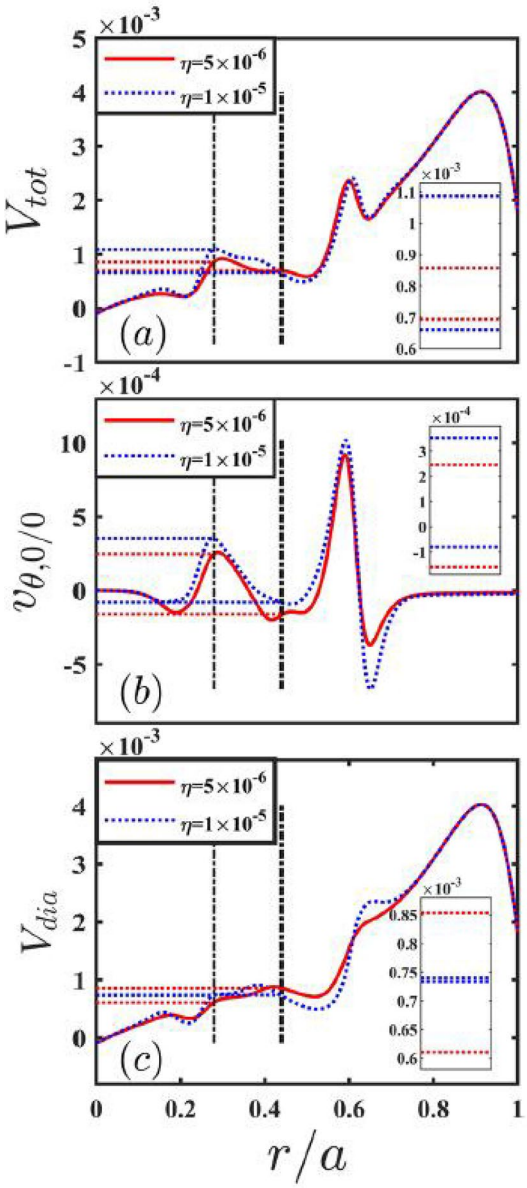

Fig. 22 The radial profile of the total flow (upper panel), zonal flow (middle panel) and electron diamagnetic flow (lower panel) within the Rutherford transition phase. The thin and thick dotted-dashed lines indicate the inner and outer rational surfaces, respectively. Reprinted from (Ye 2019)

investigated the physical properties of explosive bursts with the diamagnetic drift flow (Hu 2020). The bootstrap current is coupled into the model via modified Ohm's law as introduced in Sect. 2.2. In the simulation, the initial total current profile is fixed. The fractions of bootstrap current and the ohmic current are correspondingly adjusted to investigate different cases. Thus, the initial q-profiles are the same for different cases. We already knew that the diamagnetic drift flow can

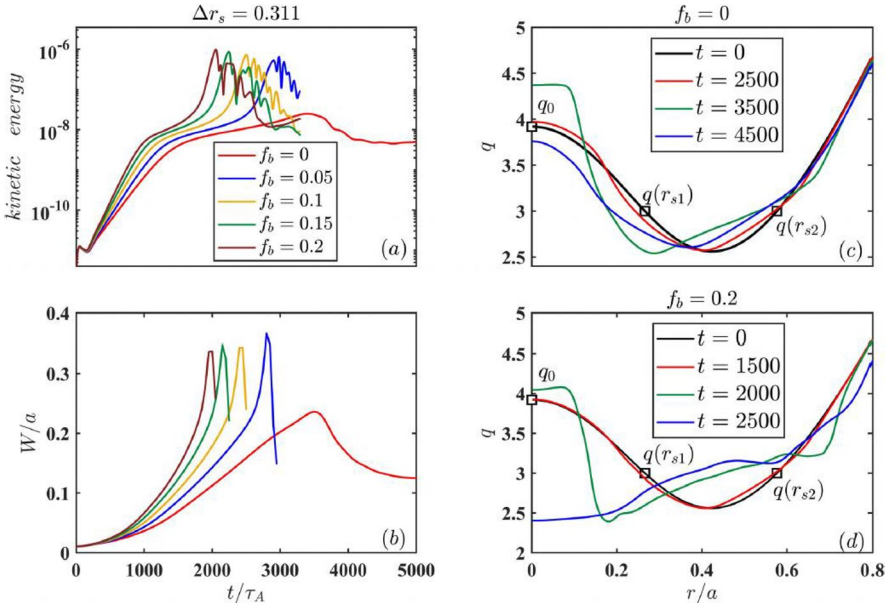

Fig. 23 Temporal evolution of **a** the $m/n = 3/1$ perturbed kinetic energy of plasma and **b** the width of the magnetic island at the outer rational surface for different bootstrap current fractions. Temporal evolution of q-profile for **c** $f_b = 0$ and **d** $f_b = 0.2$. Reprinted from (Hu 2020)

suppress the explosive burst. On the contrary, the loss of equilibrium bootstrap current will further destabilize the DTM and strengthen the explosive burst. Thus, the main question here is, to avoid the deleterious explosive burst, how these two effects (diamagnetic drift flow and loss of equilibrium bootstrap current) would compete with each other to determine the nonlinear physics mechanism in the system. Figure 23 shows that, due to the destabilizing effect of the loss of equilibrium bootstrap current, increasing its fraction would bring forward the occurrence of the explosive burst. Thus, the required amplitude of diamagnetic drift flow (corresponding to aforementioned δ_c) to suppress bootstrap current triggering explosive bursts is much larger than that in classical situations. If the separation between the two rational surfaces is enlarged, the coupling strength on both sides' islands will be impaired. Accordingly, δ_c will decline. For other key plasma parameters, the resistivity and viscosity influence the δ_c in different ways. Due to the destabilizing effect of large resistivity, the strong coupling effect will lead to a larger δ_c to completely avoid the explosive bursts than that in small resistivity regime. On the other hand, the dependence of the δ_c on the viscosity shows a nonmonotonic behavior. In the regime of small viscosity, the δ_c is proportional to the plasma viscosity due to the damping effect of viscosity on the relative rotation of islands on both sides. In the regime of large viscosity, the stabilizing effect of viscosity is the pivotal factor, and consequently just a relatively weak diamagnetic drift flow is required as viscosity increases. The impacts of the perpendicular and parallel transport coefficients on the δ_c are opposite to each other. The

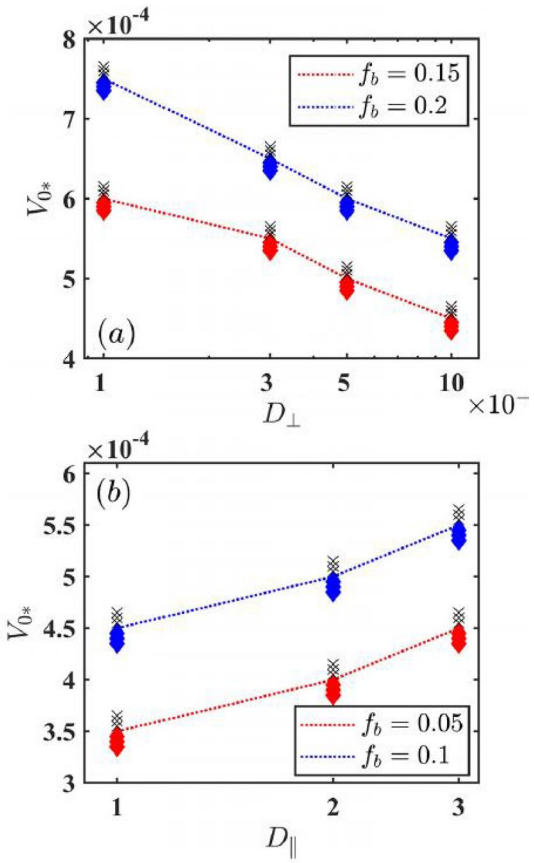

Fig. 24 The critical V_{0*c} for completely suppressing the explosive burst with **a** the perpendicular transport coefficients $D_\perp$ ($D_\parallel = 1$) and **b** the parallel transport coefficients $D_\parallel$ ($D_\perp = 1 \times 10^{-6}$). Reprinted from (Hu 2020)

improvement of parallel (perpendicular) transport coefficients would increase (decrease) the drive strength of the mode (Liu et al. 2022). Accordingly, the δ_c increases (decreases) as parallel (perpendicular) transport coefficients increase shown in Fig. 24.

6 Summary and discussion

This paper reviews recent numerical results on the nonlinear evolution and multiple control methods of NTMs in RMS tokamak plasmas, as well as the physical mechanisms behind the evolution and control processes. The studies are mainly carried out by running initial value code MDC with appropriate equilibrium according to relevant RMS experiments.

To understand the resistive MHD activities in TFTR tokamak, Wang et al. numerically investigated the nonlinear evolution of DTMs and found the evolution process included four clear phases, which are in agreement with the experimental results

(Wang 2007). The scaling law of each phase are numerically obtained and the relevant regimes are confirmed accordingly. Due to the short-pulse type discharges of TFTR, the study is limited to the physical properties of the first explosive burst. By performing a long-run simulation under advanced RMS configurations, Wei et al. reveal a type of intermittent explosive bursts triggered by self-organized fast reconnection of DTM Wei and (Wang 2014a). The physical mechanisms behind the intermittent explosive bursts are analyzed in detail. In the consideration of the multiple helicities coupling effect, Wei et al. found that the nonlinear features of multi-helicity DTMs are mainly decided by the linear unstable spectrum and the free energy volume (Wei and Wang 2014b). Once the linear growth rates of the most unstable helicity is extremely dominant, single helicity simulations are enough to contain the main nonlinear physics of the multiple helicity simulations. Otherwise, if linear growth rates of multi-helicity DTMs are in the same level, the phenomenon of consecutive explosive bursts could happen. To analyze the MHD events in JT-60U RMS experiments, Ishii et al. investigated the DTMs nonlinear evolution by adopting various initial q-profiles with different separations between the two rational surfaces. It is found that, after the Rutherford phase, the explosive bursts could be triggered in the intermediate separation cases (Ishii 2000, 2002). Based on Ishii's results, Wang et al. considered the bootstrap current effect and found that explosive bursts could be triggered with sufficiently large bootstrap current even in an extremely large separation (Wang 2015).

For controlling NTMs in various RMS configurations, Wang et al. included the differential plasma rotation into the nonlinear simulations and found the explosive burst could be effectively prevented by the differential rotation with rotation shear located in the proximity of the outer rational surface (Wang 2017). Moreover, a couple of measurable parameters are brought up according to the deformation of the magnetic islands in Rutherford phase for the prediction of the explosive burst onset. Although the predicting method works well in simulation, it is necessary to check the time scale of the response in real experiments. Considering the Alfvén time is about $10^{-6}s$ for a reactor-scale tokamak, assuming the plasma density $n_0 = 10^{20}m^{-3}$, the poloidal magnetic field at the boundary $B_0 = 0.4T$ and minor radius $a = 2.0m$. The typical time scale for the ECCD to take effect since it is turned on is less than $50ms$ (Volpe 2015). Thus, $50ms$ margin before the explosive burst is required as the real-time triangularity δ approaches the critical triangularity δ_{crit} stored in the database. Taking into account the difference of resistivity between the simulation and the real experiment, the nonlinear phase of the burst would be more than $100ms$ for the case with a large separation and a large fraction of bootstrap current. Therefore, it should work for controlling NTM islands to avoid the explosive burst via ECCD. In case of extreme situations, the δ_{crit} is recommended to be set a little smaller than that of the database during real operations. In light of the advantages of ECCD, Liu et al. attempted to apply ECCD in the suppression of NTMs and the NTMs triggering explosive bursts (Liu 2018). It is found that ECCD could be applied to effectively stabilize the NTMs as long as driven current effect is strong enough and the switch-on moment of ECCD is timely. When the neo-classical current effect is strong, the ill-advised application of ECCD could trigger the so called 'phase flip' and the following explosive bursts. Therefore, the ECCD should be turned on as early as

possible, which turns out to be feasible and effective. According to this idea, the explosive burst could also be effectively suppressed in both static islands and rotating islands situations. In experiments, however, ECCD usually is not turned on at the beginning of discharges. Thus, the real-time diagnostics such as ECEI are required to monitor the magnetic island width. Once the island width is approaching warning line, the ECCD should be turned on. Moreover, it usually takes about tens of milliseconds before the island width decreases since the ECCD is turned on (Volpe 2015). Thus, the explosive burst will not be successfully avoided if the ECCD is turned on too late. Tang et al. investigated the synergistic effects of RMP and ECCD on the control of NTMs with RMS and found that the stabilizing effectiveness and efficiency of ECCD could be further improved (Tang 2020). In the case with static RMP, the mode is locked and the continuous ECCD aiming at the O-point of the island is effective to suppress the large islands, which is similar to the situation in the experiments (Volpe 2015). Modulated ECCD is investigated in experiment to improve the effectiveness (Maraschek 2015). Enlightened by Maraschek (2015), the rotating RMP and modulated ECCD are applied. It is found that relatively small $|\omega_{ntm}/\nu|$ is favorable for the stabilizing effects of ECCD. Considering the Alfvén time is about $10^{-6}s$ in present tokamaks, a typical $|\omega_{ntm}|$ is about 6×10^{-3}, i.e., $6kHz$, $5-10$ times larger than ν in experiments. Thus, based on numerical results, to gain a better stabilizing effect, a rotating RMP with $|\omega_{rmp}| = 0.1 - 1kHz$ is encouraged to slow down the NTM. Furthermore, numerical simulation found the optimal on-duty ratio is about $60-70\%$ for modulated ECCD. In conclusion, the best control strategy is that first apply a relatively slow rotating RMP to slow down NTM islands, and then exert modulated ECCD with on-duty ratio of $60-70\%$ aiming at the inward side of initial outer resonant surface.

In the regime of high temperature, two-fluid effects could be important. Ye et al. adopted a two-fluid drift-MHD model to investigate the diamagnetic drift effect on the nonlinear evolution of DTMs (Ye 2019). It is found that the diamagnetic drift effect has a destabilizing effect on the Rutherford phase of DTMs' evolution but has a stabilizing effect on the DTM explosive bursts. The stabilizing reason is that the diamagnetic drift flow could improve the difference of rotation frequency between the two rational surfaces, which would impair the coupling effect of the DTMs' islands and thus prevent the explosive bursts. Different parameter dependence has been investigated and analyzed in both low and large viscosity regimes in detail. In terms of the effect of two-fluid on NTMs with RMS, Hu et al. extended the numerical model to consider the bootstrap current effect and investigated the influence of diamagnetic drift flow on the explosive bursts (Hu 2020). In comparison with classical situations, the required amplitude of diamagnetic drift flow to effectively avoid explosive bursts triggered by bootstrap current is much larger. As the fraction of bootstrap current increases, the critical value of diamagnetic drift flow should be improved to prevent the explosive bursts. The dependence of the critical value of diamagnetic drift flow on key plasma parameters, such as the plasma resistivity, ion viscosity and parallel/perpendicular transport coefficients, are investigated and analyzed in detail.

After years of investigations, the basic physical properties of the explosive burst have been deeply understood. The main results obtained in this paper is in

cylindrical geometry without toroidal coupling effect, which might be important in modifying the crash dynamics, although Ishii et al. found that the main properties of the nonlinear dynamics of the DTM was not changed in a toroidal geometry simulation (Ishii 2003). Moreover, multi-scale interaction between the micro-turbulence and DTM might also be significant in modifying the crash dynamics (Ishizawa 2007). For the next years, the focus should be converted into the control of explosive bursts in RMS configurations. This paper introduced several control strategies for better suppressing this type of explosive bursts based on numerical simulation results. However, other better control strategies are still necessary to be investigated due to the complexity of the realistic experimental situations. For instance, the machine learning is gradually becoming a powerful auxiliary tool in the area of plasma control recently (Liu 2020). The measurable parameters defined in (Wang 2017) might be combined with machine learning to gain a better burst prediction of effectiveness. Moreover, the experimental application of the control methods in RMS configurations should be attempted in the future. In addition, more accurate physical model which can deal with more extreme plasma parameters, such as high-beta regime (Liu 2017), two-fluid effects (Zhang 2017), and fusion born α particle physics (Wang 2021), should be established for the investigation of future burning plasma in reactor-scale tokamak devices.

Acknowledgements This work is supported by National Natural Science Foundation of China (Grant Nos. 11925501 and 12105034), the Fundamental Research Funds for the Central Universities (Grant Nos. DUT21GJ204 and DUT21LK28), China Postdoctoral Science Foundation (Grant No. 2021M690526).

Declarations

Conflict of interest On behalf of all the authors, the corresponding author states that there is no conflict of interest.

References

N. Bertelli et al., Requirements on localized current drive for the suppression of neoclassical tearing modes. Nucl. Fusion **51**, 103007 (2011)
R.J. Bickerton et al., Diffusion driven plasma currents and bootstrap tokamak. Nat. Phys. Sci **229**, 110 (1971)
D. Borgogno et al., Nonlinear response of magnetic islands to localized electron cyclotron current injection. Phys. Plasmas **21**, 060704 (2014)
R.J. Buttery et al., Neoclassical tearing modes. Plasma Phys. Control. Fusion **42**, B61 (2001)
R.J. Buttery et al., Onset of neoclassical tearing modes on JET. Nucl. Fusion **43**, 69 (2003)
H.S. Cai et al., Influence of energetic ions on neoclassical tearing modes. Nucl. Fusion **56**, 126016 (2016)
R. Carrera et al., Island bootstrap current modification of the nonlinear dynamics of the tearing mode. Phys. Fluids **29**, 899 (1986)
Z. Chang et al., Off-axis sawteeth and double-tearing reconnection in reversed magnetic shear plasmas in TFTR. Phys. Rev. Lett. **77**, 3553 (1996)
F. Crisanti et al., JET quasistationary internal-transport-barrier operation with active control of the pressure profile. Phys. Rev. Lett. **88**, 145004 (2002)
M.R. De Baar et al., Electron thermal transport barrier and Magnetohydrodynamic activity observed in tokamak plasmas with negative central shear. Phys. Rev. Lett. **78**, 4573 (1997)
D. De Lazzari et al., On the merits of heating and current drive for tearing mode stabilization. Nucl. Fusion **49**, 075002 (2009)

E.J. Doyle et al., Progress in the ITER Physics Basis. Chapter 2: Plasma confinement and transport. Nucl. Fusion **47**, S18–S127 (2007). https://doi.org/10.1088/0029-5515/47/6/S02
O. Fevrier et al., First principles fluid modelling of magnetic island stabilization by electron cyclotron current drive (ECCD). Plasma Phys. Controlled Fusion **58**, 045015 (2016)
R. Fitzpatrick et al., Helical temperature perturbations associated with tearing modes in tokamak plasmas. Phys. Plasmas **2**, 825 (1995)
T. Fujita et al., Quasisteady high-confinement reversed shear plasma with large bootstrap current fraction under full noninductive current drive condition in JT-60U. Phys. Rev. Lett. **87**, 085001 (2001)
H.P. Furth et al., Finite-resistivity instabilities of a sheet pinch. Phys. Fluids **6**, 459 (1963)
A.A. Galeev et al., Sov. Phys. JETP **26**, 233 (1968)
G. Gantenbein et al., Complete suppression of neoclassical tearing modes with current drive at the electron-cyclotron-resonance frequency in ASDEX Upgrade tokamak. Phys. Rev. Lett. **85**, 1242 (2000)
G. Giruzzi et al., Dynamical modelling of tearing mode stabilization by RF current drive. Nucl. Fusion **39**, 107 (1999)
C. Gormezano et al., Progress in the ITER Physics Basis. Chapter 6: Steady state operation. Nucl. Fusion **47**, S285 (2007)
C.M. Greenfield et al., Advanced tokamak research in DIII-D. Plasma Phys. Control. Fusion **46**, B213 (2004)
S. Günter et al., MHD phenomena in reversed shear discharges on ASDEX Upgrade. Nucl. Fusion **40**, 1541 (2000)
R. Harvey et al., Comparison of optimized ECCD for different launch locations in a next step tokamak reactor plasma. Nucl. Fusion **41**, 1847 (2001)
N. Hayashi et al., ECCD power necessary for the neoclassical tearing mode stabilization in ITER. Nucl. Fusion **44**, 477 (2004)
R.D. Hazeltine et al., A four-field model for tokamak plasma dynamics. Phys. Fluids **28**, 2466 (1985)
C.C. Hegna et al., Interaction of bootstrap-current-driven magnetic islands. Phys. Fluids B **4**, 1855 (1992)
C.C. Hegna, J.D. Callen, On the stabilization of neoclassical magnetohydrodynamic tearing modes using localized current drive or heating. Phys. Plasmas **4**, 2940 (1997)
T.C. Hender et al., MHD stability with strongly reversed magnetic shear in JET. Plasma Phys. Control. Fusion **44**, 1143 (2002)
T.C. Hender et al., Progress in the ITER Physics Basis. Chapter 3: MHD stability, operational limits and disruptions. Nucl. Fusion **47**, S128–S202 (2007). https://doi.org/10.1088/0029-5515/47/6/S03
Z.Q. Hu et al., Nonlinear mutual destabilization of the tearing mode and ion temperature gradient mode. Nucl. Fusion **54**, 123018 (2014)
Z.Q. Hu et al., Dual roles of shear flow in nonlinear multi-scale interactions. Nucl. Fusion **56**, 016012 (2016)
Z.Q. Hu et al., Suppressive effects of diamagnetic drift on neoclassical double tearing modes based on four-field reduced MHD model. Phys. Plasmas **27**, 012504 (2020)
S. Ide et al., LHCD current profile control experiments towards steady state improved confinement on JT-60U. Nucl. Fusion **40**, 445 (2000)
A. Isayama et al., Long sustainment of quasi-steady-state high β_p H mode discharges in JT-60U. Nucl. Fusion **41**, 761 (2001)
A. Isayama et al., Neoclassical tearing mode control using electron cyclotron current drive and magnetic island evolution in JT-60U. Nucl. Fusion **49**, 055006 (2009)
S. Ishida et al., Achievement of high fusion performance in JT-60U reversed shear discharges. Phys. Rev. Lett. **79**, 3917 (1997)
Y. Ishii et al., Nonlinear evolution of double tearing modes. Phys. Plasmas **7**, 4477 (2000)
Y. Ishii et al., Structure-driven nonlinear instability of double tearing modes and the abrupt growth after long-time-scale evolution. Phys. Rev. Lett. **89**, 205002 (2002)
Y. Ishii et al., Long timescale plasma dynamics and explosive growth driven by the double tearing mode in reversed shear plasmas. Nucl. Fusion **43**, 539 (2003)
A. Ishizawa et al., Excitation of macromagnetohydrodynamic mode due to multiscale interaction in a quasi-steady equilibrium formed by a balance between microturbulence and zonal flow. Phys. Plasmas **14**, 040702 (2007)
M. Janvier et al., Structure-driven nonlinear instability as the origin of the explosive reconnection dynamics in resistive double tearing modes. Phys. Rev. Lett. **107**, 195001 (2011)
Y. Kamada et al., Long sustainment of JT-60U plasmas with high integrated performance. Nucl. Fusion **39**, 1845 (1999)

R. Kamendje et al., Modeling of nonlinear electron cyclotron resonance heating and current drive in a tokamak. Phys. Plasmas **12**, 012502 (2005)
M. Kikuchi et al., Experimental evidence for the bootstrap current in a tokamak. Plasma Phys. Control. Fusion **37**, 1215 (1995)
R.J. La Haye et al., Dimensionless scaling of the critical beta for onset of a neoclassical tearing mode. Phys. Plasmas **7**, 3349 (2000)
R.J. La Haye et al., Neoclassical tearing modes and their control. Phys. Plasmas **13**, 055501 (2006)
R.J. La Haye et al., Requirements for alignment of electron cyclotron current drive for neoclassical tearing mode stabilization in ITER. Nucl. Fusion **48**, 054004 (2008)
J. Li et al., Finite frequency zonal flows in multi-scale plasma turbulence including resistive MHD and drift wave instabilities. Nucl. Fusion **49**, 095007 (2009)
X. Litaudon et al., Progress towards steady-state operation and real-time control of internal transport barriers in JET. Nucl. Fusion **43**, 565 (2003)
T. Liu et al., On the threshold of magnetic island width in nonlinear mutual destabilization of tearing mode and ion temperature gradient mode. Phys. Plasmas **23**, 102508 (2016)
T. Liu et al., Multiple MHD instabilities in high-β_N toroidal plasmas with reversed magnetic shear. Plasma Phys. Control. Fusion **59**, 065009 (2017)
T. Liu et al., Suppression of explosive bursts triggered by neoclassical tearing mode in reversed magnetic shear tokamak plasmas via ECCD. Nucl. Fusion **58**, 076026 (2018)
T. Liu et al., Control of multi-helicity neo-classical tearing modes by electron cyclotron current drive in tokamak plasmas. Nucl. Fusion **60**, 106009 (2020)
Y. Liu et al., Neural network based prediction of no-wall β_N limits due to ideal external kink instabilities. Plasma Phys. Control. Fusion **62**, 045001 (2020)
T. Liu et al., Coriolis force effect on suppression of neo-classical tearing mode triggered explosive burst in reversed magnetic shear tokamak plasmas. Chin. Phys. Lett. **38**, 045204 (2021)
T. Liu et al., Identification of multiple eigenmode growth rates towards real time detection in DIII-D and KSTAR tokamak plasmas. Nucl. Fusion **61**, 056009 (2021)
T. Liu et al., Prevention of ECCD triggering explosive bursts in reversed magnetic shear tokamak plasmas for disruption avoidance. Nucl. Fusion **62**, 056018 (2022)
T.C. Luce et al., Stationary high-performance discharges in the DIII-D tokamak. Nucl. Fusion **43**, 321 (2003)
P. Maget et al., Nonlinear magnetohydrodynamic simulation of Tore Supra hollow current profile discharges. Phys. Plasmas **14**, 0525 (2007)
M. Maraschek et al., Enhancement of the stabilization efficiency of a neoclassical magnetic island by modulated electron cyclotron current crive in the ASDEX Upgrade tokamak. Phys. Rev. Lett. **98**, 025005 (2007)
M. Maraschek et al., Enhancement of the stabilization efficiency of a neoclassical magnetic island by modulated electron cyclotron current drive in the ASDEX upgrade tokamak. Phys. Rev. Lett. **98**, 025005 (2015)
M. Murakami et al., Modification of the current profile in high-performance plasmas using off-axis electron-cyclotron-current drive in DIII-D. Phys. Rev. Lett. **90**, 255001 (2003)
S. Nishimura et al., Nonlinear dynamics of rotating drift-tearing modes in tokamak plasmas. Phys. Plasmas **15**, 092506 (2008)
C.C. Petty et al., Complete suppression of the m = 2/n = 1 neoclassical tearing mode using electron cyclotron current drive in DIII-D. Nucl. Fusion **44**, 243 (2004)
R. Prater et al., Discharge improvement through control of neoclassical tearing modes by localized ECCD in DIII-D. Nucl. Fusion **43**, 1128 (2003)
P.L. Pritchett et al., Linear analysis of the double-tearing mode. Phys. Fluids **23**, 1368 (1980)
A.H. Reiman, Suppression of magnetic islands by rf driven currents. Phys. Fluids **26**, 1338 (1983)
P.H. Rutherford et al., Nonlinear growth of the tearing mode. Phys. Fluids **16**, 1903 (1973)
Y. Sakamoto et al., Stationary high confinement plasmas with large bootstrap current fraction in JT-60U. Nucl. Fusion **45**, 574 (2005)
M. Sato et al., Study of neoclassical tearing modes based on a reduced MHD model in cylindrical geometry. Nucl. Fusion **45**, 143 (2005)
O. Sauter et al., Beta limits in long-pulse tokamak discharges. Phys. Plasmas **4**, 1654 (1997)
S. Shiraiwa et al., Formation of advanced tokamak plasmas without the use of an ohmic-heating solenoid. Phys. Rev. Lett. **92**, 035001 (2004)

A.C.C. Sips et al., Progress towards steady-state advanced scenarios in ASDEX Upgrade. Plasma Phys. Control. Fusion **44**, A151 (2002)
S. Takeji et al., J. Plasma Fusion Res. **76**, 575 (2000)
S. Takeji et al., Resistive instabilities in reversed shear discharges and wall stabilization on JT-60U. Nucl. Fusion **42**, 5 (2002)
W.K. Tang et al., Control of neoclassical tearing mode by synergetic effects of resonant magnetic perturbation and electron cyclotron current drive in reversed magnetic shear tokamak plasmas. Nucl. Fusion **60**, 026015 (2020)
A.D. Turnbull et al., Predictive capability of MHD stability limits in high performance DIII-D discharges. Nucl. Fusion **42**, 917 (2002)
K. Uzawa et al., Propagation of magnetic island due to self-induced zonal flow. Phys. Plasmas **17**, 042508 (2010)
F.A. Volpe et al., Avoiding tokamak disruptions by applying static magnetic fields that align locked Modes with stabilizing wave-driven currents. Phys. Rev. Lett. **115**, 175002 (2015)
F.L. Waelbroeck, Onset of the sawtooth crash. Phys. Rev. Lett. **70**, 3259 (1993)
X. Wang et al., Fast magnetic reconnection and sudden enhancement of current sheets due to inward boundary flows. Phys. Plasmas **3**, 2129 (1996)
Z.X. Wang et al., Fast Resistive Reconnection Regime in the Nonlinear Evolution of Double Tearing Modes. Phys. Rev. Lett. **99**, 185004 (2007)
Z.X. Wang et al., Fast linear growth of collisionless double tearing modes in a cylindrical plasma. Nucl. Fusion **51**, 033003 (2011)
X.G. Wang et al., Numerical study on the stabilization of neoclassical tearing modes by electron cyclotron current drive. Phys. Plasmas **22**, 022512 (2015)
Z.X. Wang et al., Nonlinear evolution of neo-classical tearing modes in reversed magnetic shear tokamak plasmas. Nucl. Fusion **55**, 043005 (2015)
J.L. Wang et al., Control of neo-classical double tearing modes by differential poloidal rotation in reversed magnetic shear tokamak plasmas. Nucl. Fusion **57**, 046007 (2017)
Z.R. Wang et al., Identification of multiple eigenmode growth rates in DIII-D and EAST tokamak plasmas. Nucl. Fusion **59**, 024001 (2019)
F. Wang et al., PTC: full and drift particle orbit tracing code for α particles in tokamak plasmas. Chin. Phys. Lett. **38**, 055201 (2021)
Z.X. Wang et al., A brief review: effects of resonant magnetic perturbation on classical and neoclassical tearing modes in tokamaks. Plasma Sci. Technol. **24**, 033001 (2022)
L. Wei et al., A mode transition in self-suppressing double tearing modes via Alfvén resonance in rotating tokamak plasmas. Nucl. Fusion **51**, 123005 (2011)
L. Wei et al., Numerical study of collisionless q=1 double tearing instability in a cylindrical plasma. J. Plasma Phys. **78**, 663 (2011)
L. Wei, Z.X. Wang, Intermittent bursts induced by double tearing mode reconnection. Phys. Plasmas **21**, 062505 (2014)
L. Wei, Z.X. Wang, Nonlinear evolution of double tearing modes in tokamak plasmas via multiple helicity simulation. Nucl. Fusion **54**, 043015 (2014)
E. Westerhof et al., Closure of the single fluid magnetohydrodynamic equations in presence of electron cyclotron current drive. Phys. Plasmas **21**, 102516 (2014)
C. Ye et al., Effects of diamagnetic drift on magnetohydrodynamic explosive bursts in reversed magnetic shear tokamak plasmas. Nucl. Fusion **59**, 096044 (2019)
Q. Yu, Nonlinear evolution of neoclassical double tearing mode. Phys. Plasmas **4**, 1047 (1997)
Q. Yu et al., Stabilization of neoclassical tearing modes by an externally applied static helical field. Phys. Rev. Lett. **85**, 2949 (2000)
Q. Yu et al., Interactions between neoclassical tearing modes. Nucl. Fusion **40**, 2031 (2000)
Q. Yu et al., Numerical studies on the stabilization of neoclassical tearing modes by radio frequency current drive. Phys. Plasmas **11**, 1960 (2004)
Q. Yu et al., Linear and nonlinear stability of drift-tearing mode. Nucl. Fusion **50**, 025014 (2010)
Q. Yu, S. Günter, Numerical modelling of neoclassical double tearing modes. Nucl. Fusion **39**, 487 (1999)
W. Zhang et al., Hall effect on tearing mode instabilities in tokamak. Phys. Plasmas **24**, 102510 (2017)
W. Zhang et al., Core-crash sawtooth associated with m/n= 2/1 double tearing mode in tokamak. Plasma Phys. Control. Fusion **61**, 075002 (2019)

W. Zhang et al., Influence of shear flows on dynamic evolutions of double tearing modes. Nucl. Fusion **60**, 126022 (2020)
W. Zhang et al., The off-axis pressure crash associated with the nonlinear evolution of the m/n = 2/1 double tearing mode. Phys. Plasmas **27**, 122509 (2020)
H. Zohm, Stabilization of neoclassical tearing modes by electron cyclotron current drive. Phys. Plasmas **4**, 3433 (1997)
H. Zohm et al., The physics of neoclassical tearing modes and their stabilization by ECCD in ASDEX Upgrade. Nucl. Fusion **41**, 197 (2001)
H. Zohm et al., Control of MHD instabilities by ECCD: ASDEX Upgrade results and implications for ITER. Nucl. Fusion **47**, 228 (2007)